Traffic & Transportation

Wireless Channel Propagation Model for Inland Waterway Bridge Scenario

Yi ZHANG[1], Wenfei HU[2], JunWu ZHANG[2], Jing ZHANG[3]

Original Scientific Paper
Submitted: 18 Jan 2024
Accepted: 29 Mar 2024

[1] 202110110404@ctgu.edu.cn, Three Gorges University, Computer and Information Engineering College
[2] wenfeihu@ctgu.edu.cn, Three Gorges University, Computer and Information Engineering College
[2] zhang_junwu@ctg.com.cn, Three Gorges Corporation, Three Gorges Ecological Environment Co.
[3] Corresponding author, zhangjing3@ctgu.edu.cn, Three Gorges University, Hubei Key Laboratory of Intelligent Vision Based Monitoring for Hydroelectric Engineering

Publisher:
Faculty of Transport and Traffic Sciences, University of Zagreb

ABSTRACT
Intelligent shipping is a crucial part of the transportation system, while inland river intelligent shipping is a major safeguard of intelligent transportation. Compared with the studies of mobile fading channels in land-based environments, less current research has focused on channel measurements and modeling for inland waterway bridge environments. In this paper, a segmenting radio channel model is proposed for inland highway and railway combined bridges. The ship's path under the bridge was divided into three phases, and the attenuation of signal strength was modelled separately for each. Hence, it shows ship-to-ship wireless channels in different areas and path loss on inland navigation bridges. A segmented model, instead of a basic path loss model, can accurately forecast path loss and provide a practical approach in ship-to-ship wireless channel transmission scenarios over bridges. Consequently, the channel measurements and modeling in the typical inland waterway are of great significance for establishing a reliable inland navigation broadband radio communication system.

KEYWORDS
ship-to-ship; wireless communication; inland waterway; wireless channel property; wireless channel modeling.

1. INTRODUCTION

Ship-to-ship (S2S) wireless communication systems are crucial for supporting the development of intelligent transport in inland waterways. Inland waterway intelligent transport system (IWITS) uses information, communication and control technology to improve interaction and collaboration between inland and land transport. IWITS's primary objective is to enhance navigation safety, efficiency and environmental sustainability.

In recent years, plenty of research on wireless S2S communication systems has been carried out and has received much attention [1–3]. The purpose of these measurements is to acquire a better understanding of the statistical properties of the S2S propagation channel. Papers [4–6] provided extensive propagation properties of water surfaces, particularly under non-line-of-sight (NLOS). Loss, Doppler spread analysis and small-scale fading distributions on suspension and beam bridge conditions can be found in paper [7]. However, channel characteristics that are suitable for IWITS environments are still lacking. Previous inland waterway channel measurements have mainly focused on fixed ship-to-land performance. Paper [8] presents a measurement analysis of the wireless propagation channel near the Amazon River at a frequency of 5.21 GHz. The coherence of wave propagation in the transition region is comparatively examined. Paper [9] discusses the loss of signal strength in the wireless channel when transmitting at various distances. There is a 19 dB difference between different propagation modes in the VHF band of radio waves. These measurements were taken in urban, inland

waterway and forest environments. Paper [10] examines the channel eigenvalues and compares them to the observed channel eigenvalues using the Okumura-Hata model theory. This analysis determines the measured distance cut-off point for inland waterways, which helps differentiate between LOS and NLOS scenarios.

Although these studies exist, researchers must thoroughly treat inland waterway bridge wireless (IWBW) channel measurements. Accurate IWBW measurements are crucial in analysing IWITS [11–12]. Nevertheless, IWBW demonstrates notable distinctions compared to traditional networks. Hence, various inland waterway environments and navigational circumstances on radio wave propagation significantly contribute to developing the IWBW network. This work has revealed several factors responsible for multipath propagation, antenna characteristics, surface reflections and various inter-vessel navigation scenarios [13–14]. Therefore, within the realm of inland navigation, conducting thorough IWBW measurements is essential.

To research the path loss modelling of IWBW, dividing the S2S communication links into three distinct classes is essential. So, the IWBW path loss model should be thoroughly analysed.

1) Free-space region (FS): It is the situation when the ship approaches the bridge. The IWBW demonstrates that the ship-bridge distance influences free space path loss characteristics.
2) Bridge-hole region (BH): It is the situation when the ship passes under the bridge. Multipath propagation issues predominantly impact the IWBW in a specific location. Different environmental entities, such as bridge structures, lead to signal and path loss fluctuations due to multiple reflection, diffraction and scattering events.
3) Distant-space region (DS): It is the situation where the ship continues sailing after crossing the bridge. Examining the IWBW path loss as a distinct entity is imperative to ascertain the diffraction loss in DS. Hence, comprehensive research of the IWBW path loss model can be performed by dividing the S2S communication links into these three categories and accounting for the unique features of each group.

The main contribution of this paper lies in enhancing the wireless channel model situated in various shaded regions, using the deterministic modelling method and segmented architecture. The IWBW model for inland waterway bridge scenarios is proposed and the effect of the wireless propagation channel is investigated in conjunction with bridge shadow fading. The methodological approach in this research is a modelling methodology based on the radio wave propagation mechanisms to various geographical areas. This IWBW model takes into account the bridge box area and the distant area, and more fully reflects the prediction of radio wave transmission loss of inland waterway shipping in the bridge scene. The rest of the paper is organised as below. Section 2 presents a concise overview of the IWBW path loss measurements. This step defines the preliminary stage in formulating a wireless channel model tailored explicitly for IWBW. Section 3 elaborates on the channel model. The examination and analysis of the validation outcomes of the model are shown in Section 4, employing the root mean square error algorithm. Section 5 concludes the paper.

2. CHANNEL MEASUREMENTS

2.1 Measurement equipment

The measurement system mainly contained the transmitter (TX) part, receiver (RX) part, a wireless channel measuring device, a time-division multiplexing (TDM) channel detector, laptops, power supplies, a marine speedboat, a landing stage, automatic identification system (AIS) and global positioning system (GPS). Measurements were obtained using a time-division multiplexing (TDM) channel sounder provided by the Norwegian Institute to test the IWITS channel characteristics. The TDM operates at a central frequency of 5.9 GHz and employs a linear frequency modulation signal with a bandwidth of 100 MHz, repeated at a specific rate. The equipment transmits a specified signal level and acquires channel data by analysing the signals received from RX. The channel sounder mainly consisted of the TX and RX. An omnidirectional vertical antenna for TX antenna and a directional vertical antenna for RX antenna is used, as shown in *Figure 1b and Figure 1d*. According to traditional wireless propagation channels research for S2S communication in IWITS [2], TX and RX antennas tend to be higher than bridges. However, the current paper adopts that the TX and RX antennas have a lower height than the bridges.

TX platform: It employs a marine speedboat, as shown in *Figure 1a*. The vertical distance between the antenna platform and the water's surface is about 4 m, while the TX antenna is about 4.6 m above the water's level. TX emits 100 MHz bandwidth chirp signal with 10 ns delay resolution and 16 dBm TX power. The ship's position and radio signal data are linked to the transmitter's portable computer via RJ45 port.

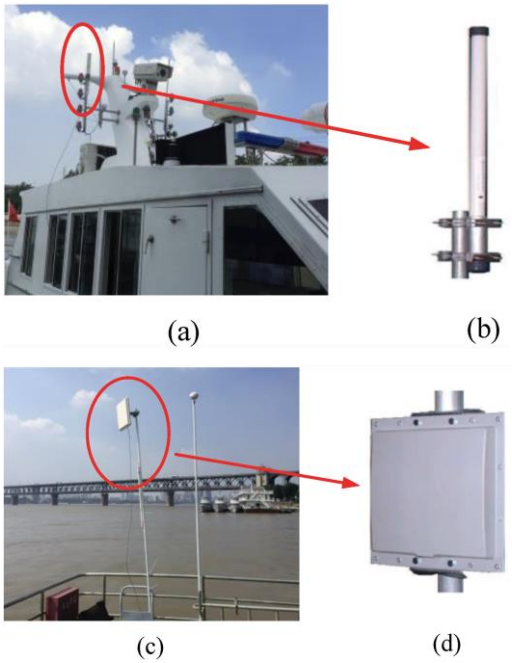

Figure 1 – Types and installation of antennas: TX antenna: (a) ship platform installation (b) omnidirectional vertical antenna; RX antenna: (c) pontoon platform installation (d) directional vertical antenna

RX platform: It employs a landing stage anchored at the bank of an inland waterway. The RX antenna is positioned on this platform, as shown in *Figure 1c*. It is a vessel that lacks propulsion capabilities and is commonly found in the harbours of cities located along inland waterway. A vertical directional receiving antenna with 16 dBi gain (3 m height) has a receiving antenna lobe width azimuth angle of ±45°. The RX antenna is linked to a computer to record all measurement data via RJ45 port.

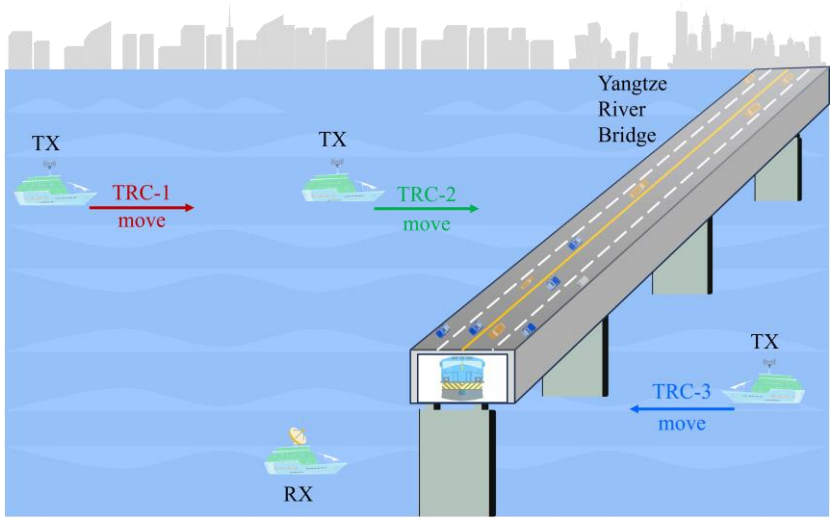

Figure 2 – The structure of the measurement scenario and TX and RX predefined positions

Three distinct wireless transmission channel measurement scenarios were devised, namely TX-RX wireless channel measurement scenery 1(TRC-1), TRC-2 and TRC-3, shown in *Figure 2*, to evaluate the influence of bridges on IWBW. All three scenario partitions are made with the bridge S2S in different locations using the bridge as a reference. TRC-1 includes the absence of bridges and the vessel operating under standard navigation conditions. To examine the impact of the bridges on wireless signal transmission, TRC-1 is established as the baseline scenario for comparison with TRC-2 and TRC-3 to assess the level of signal degradation in the IWITS system. The crossing of the bridge involves two scenarios: TRC-2 and TRC-3. In TRC-2, the TX ship moves away from the RX ship. In TRC-3, the TX ship travels toward the RX ship. The TX with an omnidirectional antenna mounted on the ship moved at a uniform speed. The RX ship is stationary on the waterway shoreline, with zero velocity. All of the measurement parameters are presented in *Table 1*.

Table 1 – Measurement system parameters

Parameters	TRC-1	TRC-2	TRC-3
Carrier frequency	5.9 GHz	5.9 GHz	5.9 GHz
Delay resolution	10 ns	10 ns	10 ns
Sample number	2560/chirp	2560/chirp	2560/chirp
TX antenna type	Omni-directional vertical	Omni-directional vertical	Omni-directional vertical
RX antenna type	Directional vertical	Directional vertical	Directional vertical
RX antenna lobe width azimuth angle	±45°	±45°	±45°
RX height	5.0525 m	5.0525 m	5.0525m
TX height	4.61 m	4.61 m	4.61 m
TX power	16 dBm	16 dBm	16 dBm
TX gain	10 dBi	10 dBi	10 dBi
RX gain	16 dBi	16 dBi	16 dBi
Measuring time	8 s	8 s	9 s
TX sailing distance	110 m	110 m	110 m
TX-RX distance	840-760 m	760-840 m	770-695 m

2.2 Other structural paper elements

The 5.9 GHz measurement campaign was conducted in a highway and railway combined bridge in the Wuhan section of the Yangtze River. The bridge structure features a double-deck design, with the lower chord beams of the main truss serving as the railway deck and the upper chord beams as the road deck. It was noted that the lowermost point of the bridge exhibited an approximate vertical distance of 20 meters from the sea surface. In comparison, the horizontal span between the piers was estimated to be around 128 meters. To enhance our comprehension of ship traversal across a bridge, we studied the cross-sectional illustration of a ship's passage through a bridge, as shown in *Figure 3*.

The system for measuring IWBW used for S2S communication is shown in *Figure 4*. The radio wave propagation on the water surface of the inland waterway is influenced by several factors, including the curvature of the Earth, the distance between the TX and RX antennas and the reflection from the water surface (as shown in *Figure 5* and *Table 2*) when the TX ship passes under the bridge. As shown in *Figure 5*, many signal transmission pathways exist between the TX and RX when a vessel traverses a bridge aperture. In addition to the primary trajectory of the beam, notable reflections take place within a brief timeframe, encompassing reflections between piers and the water surface, as well as reflections involving bridge piers and the water surface. Hence, we designated the bridge, the bottom section of the dock and the horizontal plane as a spatial enclosure resembling a tunnel, denoted as the bridge box.

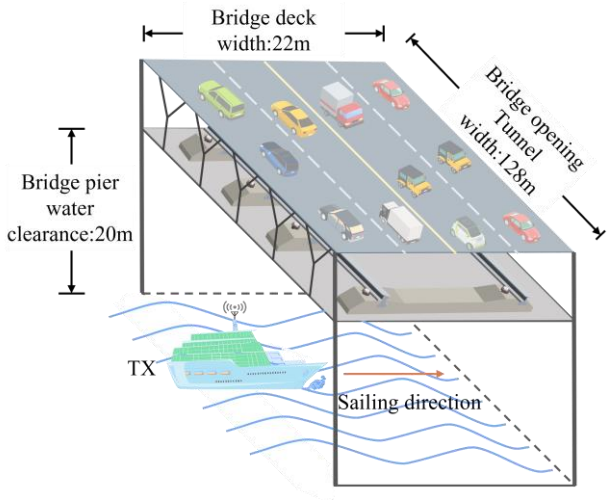

Figure 3 – Inland bridge scene cross-section and TX travelling downstream across the bridge hole.

A multipath effect affecting the RX signal is subject to several factors, including reflections from the ocean surface, reflections from the bridge pier and the bridge surface, shadowing effects within the bridge box, and repeated reflections. Shadowing effects within the bridge box further contribute to the overall impact on IWBW. Repeated reflections result in energy losses for radio waves. Reflections originating from the water surface can lead to substantial fluctuations in the IWBW path loss.

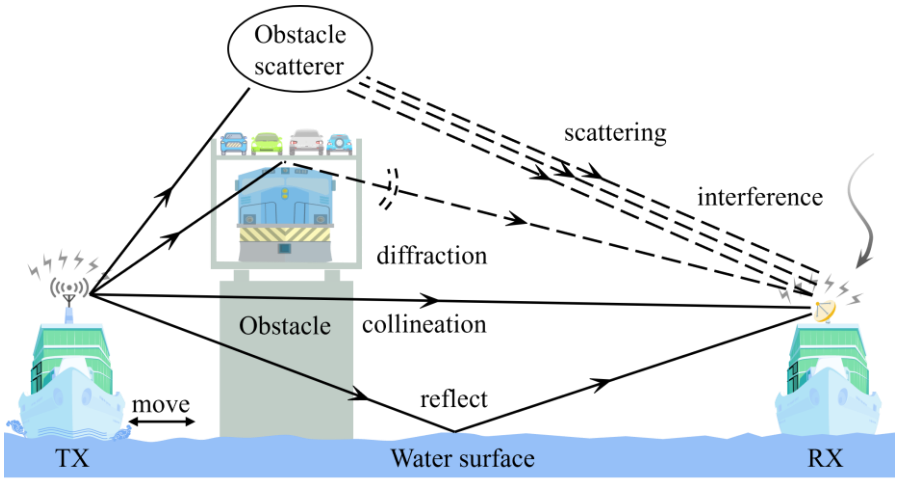

Figure 4 – Test system and measurement scenario for inland waterway

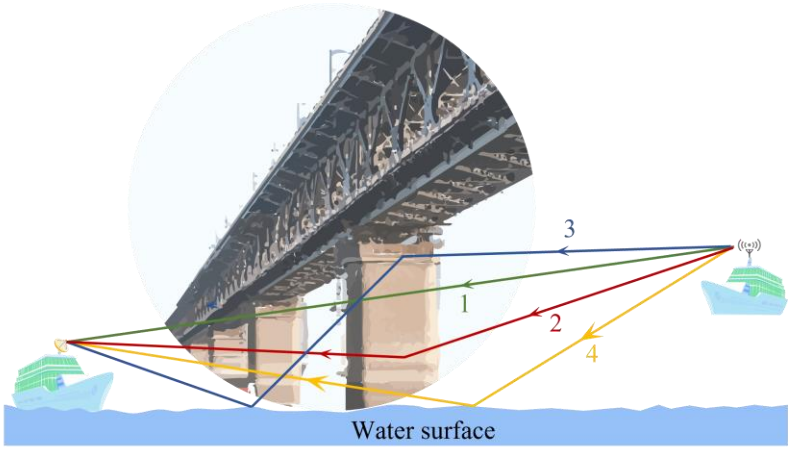

1: Direct path
2: Bridge pier reflection
3: Abutment - water surface specular reflection
4: Water surface reflection
5: Bridge bottom - water surface specular reflection
6: Bridge bottom - abutment reflection
7: Bridge bottom - abutment - water surface reflection

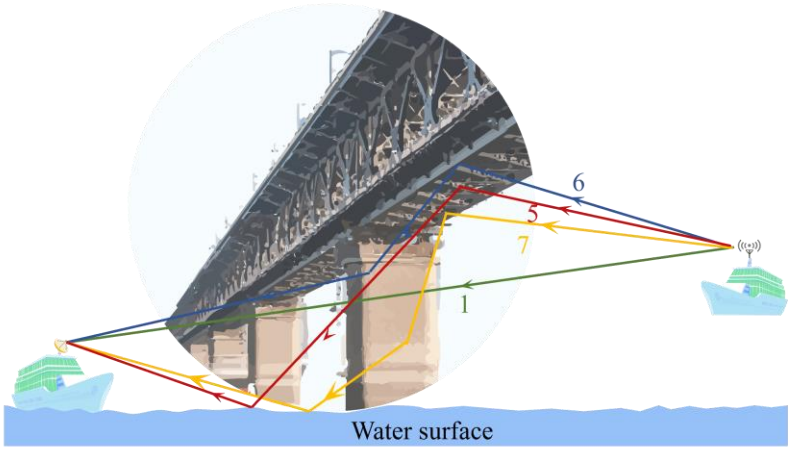

Figure 5 – Measurement route and propagation path loss analysis

Table 2 – Bridge scene ship-ship radio wave main propagation mechanisms

	Radio wave main propagation mechanisms	Number of reflections*
1	Direct path	-
2	Bridge pier reflection	1
3	Abutment - water surface specular reflection	2
4	Water surface reflection	1
5	Bridge bottom - water surface specular reflection	2
6	Bridge bottom - abutment reflection	2
7	Bridge bottom - abutment - water surface reflection	3

** Number of reflections is the number of reflections this propagation mechanism experiences.*

3. MEASUREMENT RESULTS

This section will measure and analyse the path loss versus the TX-RX separation distance for IWBW, as shown in *Figure 2*, *Figure 6*, *Table 3* and *Table 4*. The TRC-1 wireless channel transmission without any bridge interference can be shown in *Figure 6a*. *Table 3* presents the summary statistics for the rise of signal attenuation with the expanding TX-RX separation distance and some obstacles. The signal power for TRC-1 ranged from 87.34 to 92.29 dB, and the mean value was 89.96 dB. There was a significant positive correlation between path loss and distance for the LOS case.

Nevertheless, a notable disparity in the TRC-2 and TRC-3 path loss is shown in *Figures 6b* and *6c* when a TX vessel traverses a bridge, compared to TRC-1. In the TRC-2, the IWBW path loss remains consistent as the TX-RX separation distance increases. According to *Figure 6b*, there is a clear trend of decreasing from 92.28 dB to 91.03 dB when the TX ships cross the bridge. However, the signal steady attenuation escalates from 91.03 dB to 92 dB with the increasing TX-RX separation distance as a vessel traverses a bridge. Therefore, large obstacles in the inland waterway have a notable influence on the IWBW parameters, with the constant TX-RX distance, comparing the path loss between TRC-1 and TRC-2. Furthermore, TRC-3 dramatically fluctuated data, indicating that the BH region and bridge abutments caused strong reflections on the radio propagation channel, resulting in a multipath effect on the RX antenna.

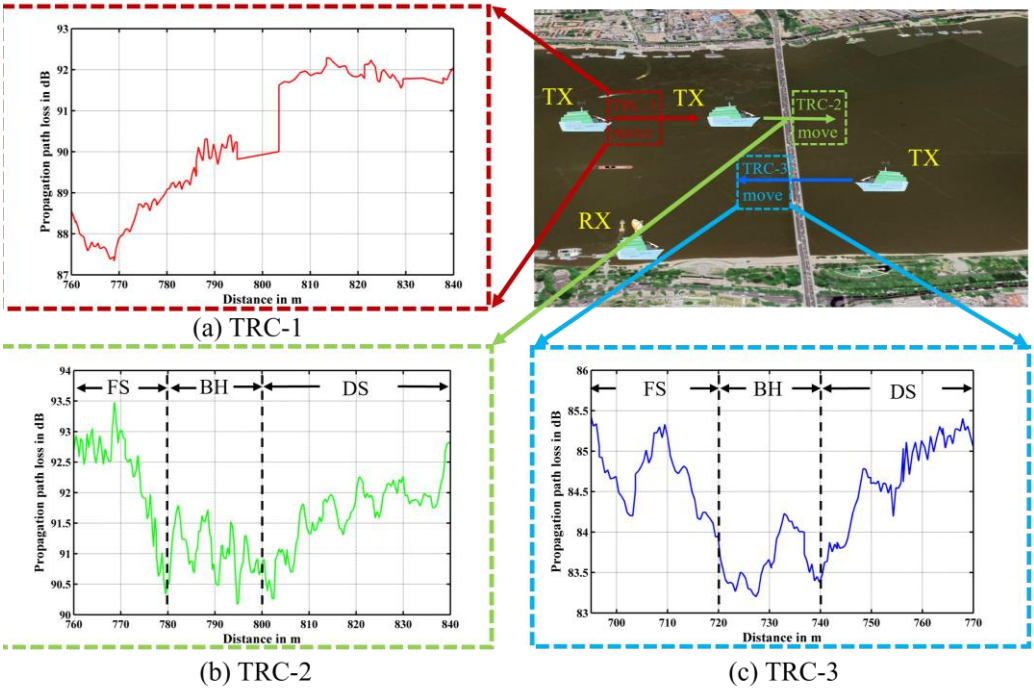

Figure 6 – Path loss analysis of bridge scene

Table 3 – Path loss measurement in bridge scenario

	Min (dB)	Max (dB)	Mean (dB)	Standard deviation (dB)
TRC-1	87.34	92.29	89.96	1.66
TRC-2	90.17	93.48	91.64	0.73
TRC-3	83.20	85.00	84.37	0.62

Table 4 – Path loss measurement under bridge

	Min (dB)	Max (dB)	Mean (dB)	Standard deviation (dB)
TRC-2	90.17	91.79	91.63	0.37
TRC-3	83.20	84.23	83.64	0.30

Figure 6b, *Figure 6c*, *Table 3*, *and Table 4* show apparent changes when the TX ship traverses the bridge in different directions relative to the RX ship. The average path loss of TRC-2 is approximately 7.27 dB higher than that of TRC-3, shown in *Table 3*. These path-loss changes imply that the TX ship orientation significantly impacts the wireless channel parameters, direct path and strongly reflected components between the TX and RX antennas.

In addition, TRC-1 has an average path loss of roughly 1.95 dB lower than TRC-2, and TRC-1 has an approximately 5.59 dB higher path loss than TRC-3. Hence, there are still some disparities in wireless communication between ships. *Table 4* shows that the difference between the pass-through loss of TRC-2 and TRC-3 under the bridge is about 8db. So, when the boat passes through the bridge, in addition to the TX-RX spacing and the influence of water surface reflections, the internal reflections of the BH region strongly influence RX.

The path loss remains essentially constant regardless of the TX-RX separation distance in the bottom space of the bridge. There is a vast reflective space inside the bridge box to form a scatterer, which significantly impacts the radio wave transmission. The simple path loss model cannot meet the transmission of radio waves in the bridge scenario and the prediction of the bridge scenario.

Consequently, typical geometric space-based exponential models do not apply to IWBW. Three stages must be made: the ship approaches the bridge, passes under it and continues after crossing it. Therefore, inland waterway bridge scenario models must consider the effects of water surface reflections, abutment reflections and shadow decay under bridges.

4. PATH-LOSS CHANNEL MODELLING

Many reflection considerations must be addressed when traversing a bridge obstacle in an inland canal. Based on the earlier analysis and extensive measured data, the propagation path of a ship via a bridge hole has been separated into three sections, namely the free-space region (FS), bridge-hole region (BH), and distant-space region (DS), as shown in *Figure 7* as follows:

1) FS: The IWBW generally consists of LOS paths, where the transmission path loss is impacted by water surface reflection and changes in the TX-RX separation distance. A IR model in paper [15] can be effectively applied to the FS region section of our report. Compared with the REL model, this model shows three improvements from inland river scenario differences.
2) BH: Radio waves are reflected more than once in a bridge box, leading to superposition and multi-path effects. The radio wave transmission also varies significantly due to changes in the TX-RX separation distance and reflection off the water's surface. From *Figures 3* and *4*, ships moving through the bridge are regarded as travelling through a short tunnel in a short time. As a result, the radio wave transmission between ships and the attenuation of multiple radio wave reflections need to be considered.

$$PL_{BHL}=32.44\text{dB}+20\lg PL+20\lg F(MHz)-10\lg(GtGr)-20\lg\left|1+\sum_{i=1}^{M}\sum_{P_L}^{Ni}\prod_{k=1}^{i}\Gamma i P_L k e^{j\Delta\varphi_i P_L}\right| \quad (1)$$

Here, PL_{BHL} represents the BHL model. i reflects the number of the type of reflections it undergoes, with a total of M reflections. F denotes the center frequency in 5.9 GHz. PL represents the radio wave reflection

paths, with N_i paths for each reflection, and the total length of each propagation path is $\sum_{a=1}^{i+1} L_{l_a}$. k reflects the traits of reflections on each path, $\Gamma i P_L k$ denotes the reflection coefficient of each radio wave inflection, and $\Delta\varphi_{iL_r}$ represents the phase difference between the direct path and the P_L path of the radio wave reflection. The

$$PL_{BH} = R_r PL_{BHL,T_{d1}} - \kappa \sum_{i=1}^{n} \left(T_{d_i} - T_{d_1}\right) \tag{2}$$

model for the BH region is derived as follows:

PL_{BH} represents the wireless propagation channel loss model in the BH region. R_r is the freshwater reflection coefficient of inland waterways [16-17]. $PL_{BHL,T_{d1}}$ represents the TX radio wave path loss at the turning point T_{d_1}, and T_{d_i} is the TX-RX separation distance when the ship is within the bridge hole. κ represents the attenuation factor of wireless radio waves in the bridge hole space in dBm.

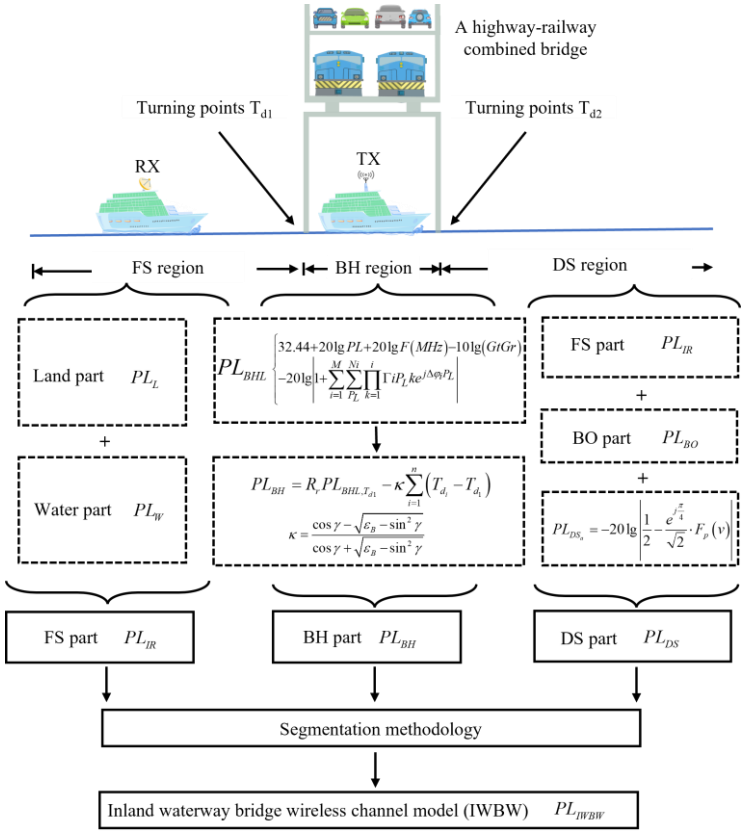

Figure 7 – The structure of the inland waterway bridge wireless channel model

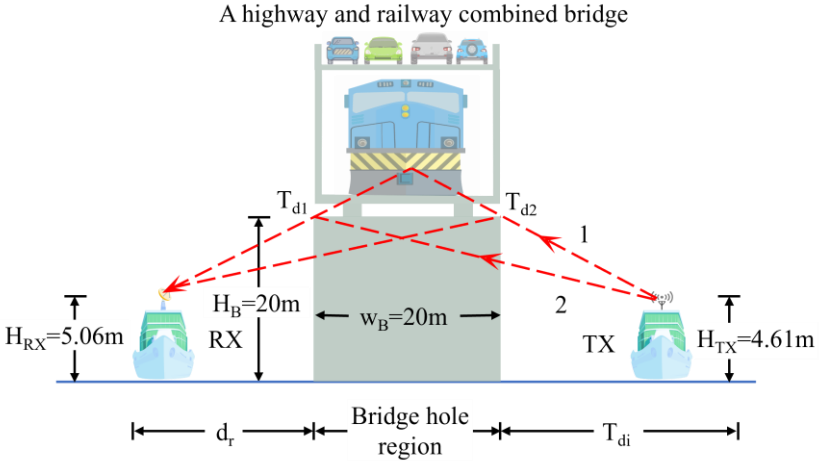

Figure 8 – Analysis of wireless signal diffraction propagation path above the bridge

Therefore, this experiment adopts geometrical analysis to analyse the radio wave reflected inside the bridge box to reach the RX antenna shown in *Figures 3* and *5*. Direct and multiple reflection paths exist between the TX and RX antennas. So, the Bridge Hole Loss model (BHL) is expressed as follows below.

By geometric theory [18], the following physical equation can be used to represent the attenuation factor for scenarios involving bridges and tunnels in urban settings;

$$\kappa = \frac{cos\gamma - \sqrt{\varepsilon_B - sin^2\gamma}}{cos\gamma + \sqrt{\varepsilon_B - sin^2\gamma}} \tag{3}$$

ε_B represents the relative permittivity of the bridge piers and structures, γ is the angle of radio wave incidence.

(3) DS: T_{d_2} denotes the second turning point after the ship traverses the bridge hole shown in *Figure 7*. TX-RX wireless propagation channel analysis needs to consider direct radio wave emission through the BH region, reflections from inside the bridge box, reflections from the water surface, radio waves circling above the bridge because of the TX-bridge-RX position relationship.

Significant signal attenuation happens because bridge obstructions impede the ability to transmit signals when ships navigate into the DS region. Nevertheless, the RX antenna can still capture radio waves due to the diffraction phenomenon. Because the TX and RX antennas have a lower height than the bridges, the propagation channel situation above the bridge should be computed to obtain the IWBW diffraction loss as shown in *Figure 8*. This paper investigates diffraction losses in radio propagation channels within the inland waterway FS region, drawing upon the Deygout calculation method [19].

It is worth noting that the impact of the bridge surface and pier thickness on radio wave propagation is disregarded. "1" and "2" represent the diffracted rays generated on the edge cross-section of the bridge at T_{d_2} and T_{d_1} shown in *Figure 8*, respectively. According to the Deygout calculation method, PL_{DS_a} of radio wave diffraction loss over bridges can be expressed as:

$$PL_{DS_a} = -20lg\left|\frac{1}{2} - \frac{e^{j\frac{\pi}{4}}}{\sqrt{2}} \cdot F_p(v)\right| \tag{4}$$

where v represents the Fresnel parameter. According to the Deygout method, $F_p(v)$ can be defined as:

$$F_p(v) = \int_0^v e^{-j\cdot\pi\left(\frac{t^2}{2}\right)}\,dt \tag{5}$$

Fresnel parameter v can be expressed as:

$$v = \theta_{T_{d_1}}\sqrt{\frac{2}{\lambda\left(d_{T_{d_i}}^{-1} + w_B^{-1}\right)}} \tag{6}$$

$\theta_{T_{d_1}}$ represents the diffraction radio wave angle at T_{d_1} when radio waves travel from TX to the edge angle T_{d_2} of the bridge. $\theta_{T_{d_1}}$ is given by:

$$\theta_{T_{d_1}} = \frac{\pi}{2} - arctan\frac{T_{d_i}}{H_B - H_{TX}} \tag{7}$$

H_B denotes the height of the bridge piers (20 m), and H_{TX} is the height of the TX ship (4.61 m).

Inland navigation wireless communication has three propagation regions, FS, BH, DS, and other multiple reflection and scattering situations. Therefore, the effects caused by multiple reflections and attenuation of the increased radio waves on the receiving antenna are neglected. In the IWBW research, the propagation paths are mainly considered free-space propagation, reflection from the bridge box, and diffraction over the bridge. Therefore, the model should be appropriately corrected according to the diffraction loss of the wireless propagation channel in the actual DS region, and the wireless propagation channel attenuation model can be expressed as follows:

$$PL_{DS}=PL_{IR} + PL_{BH}+PL_{DS_a} \tag{8}$$

PL_{DS} represents the loss model for wireless propagation channels in the bridge scenario DS region.

By combining *Equations 1–8*, the segmented IWBW model can be summarised as follows:

$$PL_{IWBW} = \begin{cases} PL_{IR} \\ PL_{BH} = R_r PL_{BHL,T_{d_1}} - \kappa \sum_{i=1}^{n} (T_{d_i} - T_{d_1}) \\ PL_{DS} = PL_{IR} + PL_{BH} + PL_{DS_a} \end{cases} \quad (9)$$

5. MEASUREMENT RESULTS

Root-mean-square error arithmetic is used to verify the model. The experiment assumes that the TX ship sails along the centre line of the bridge hole. The incident angle of the radio wave on the pier and the water surface is 45°. When the TX ship sails in TRC-2, the reflection number of the radio wave propagation mechanisms undergoing inside the bridge box is assumed to be 0-10. When sailing in TRC-3, the reflection number of the radio wave propagation mechanisms undergoing inside the bridge box is considered 0-2.

Satellite pictures and path loss models are provided as shown in *Figure 9*. In *Figure 9a*, the red dots show route loss measurements for TRC-2, the blue line represents the PL_{IR} model, the pink line represents the PL_{BH} model, and the black line is the PL_{DS_a} model. In *Figure 9b*, the red dots show route loss measurements for TRC-3, the blue line represents the PL_{IR} model, the pink line represents the PL_{BH}model, and the black line is the PL_{DS_a} model.

All three models can match the actual IWBW path loss, as shown in *Figure 9*. As a ship navigates in TRC-2, there is a significant difference between the IWBW path loss model and the free space propagation model. The wireless propagation channel characteristics tend to be within an oscillating interval because of the superposition of solid reflections caused by the BH region. The reflection impact from the bridge box is small when TX sails in TRC-3. Path loss and antenna spacing are the main factors. According to *Tables 5 and 6*, the mean error of the two models approaches 0, and the root mean square error is lower than 5. Further analysis showed that the segmentation model could generate large-scale path loss prediction for inland waterway bridges because the design of this model was based on bridge box reflections and the Deygout approach.

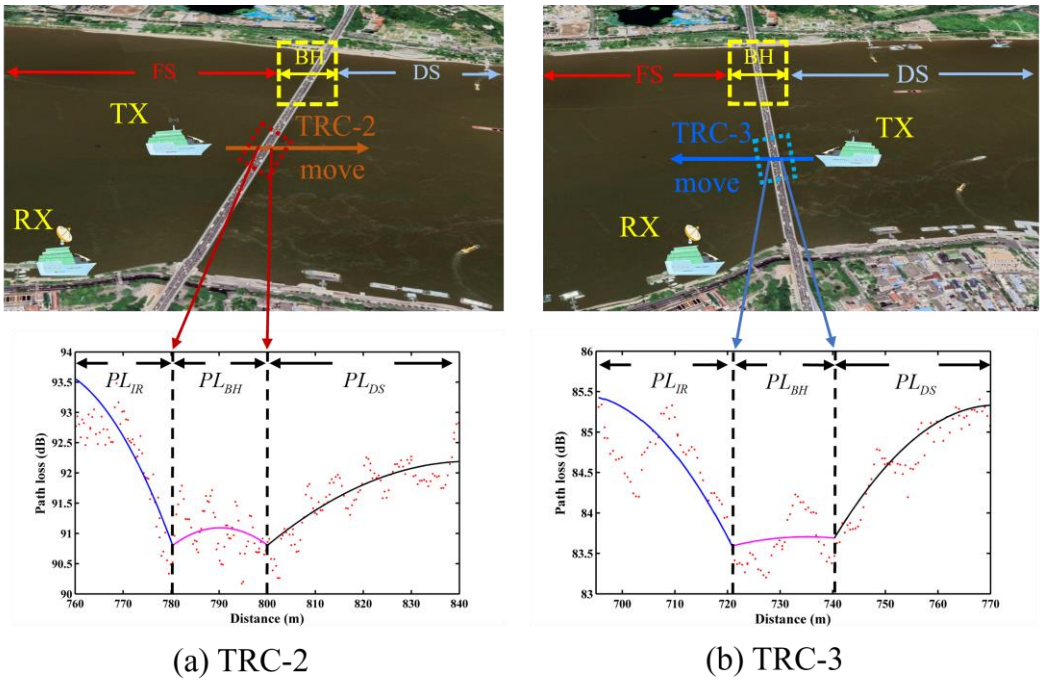

Figure 9 – A segmented model of large-scale path loss for ships sailing through different areas of bridges

Table 5 – Comparison of TRC-2 measured values with model values

Error \ Model	BH loss model	BD loss model
Mean error (dB)	0.2	0.35
RMS error (dB)	3.73	4.42

Table 6 – Comparison of TRC-3 measured values with model values

Error \ Model	BH loss model	BD loss model
Mean error (dB)	0.32	0.26
RMS error (dB)	5.0	2.52

6. MEASUREMENT RESULTS

This paper offers a segmented wireless channel propagation model in an inland waterway, which incorporates a separation between free space region, bridge tunnel area and remote area. The verification of our model through a comparison with our measurement data shows its capacity to reflect the actual S2S wireless channel characteristics in different regions and anticipate the radio wave path loss in the inland waterway bridge scene. In the past, despite most studies in path loss models having only focused on the terrestrial environment, the influence of the inland waterway bridge environment on S2S wireless channels has largely been disregarded. Thus, a segmented model can provide a practical approach in ship-to-ship wireless communication in a bridge environment and it paves the way for designing better S2S wireless communication systems for next-generation IWITS applications.

ACKNOWLEDGEMENTS

The authors would like to express their sincere thanks to Wuhan University of Technology (WHUT) for supporting the data analysis and to the Wuhan Changjiang Waterway Engineering Bureau for their coordination work during the measurement process. The work was supported by the Research on Key Technology of Inland Waterway Ship Navigation Based on Visual Perception and Enhancement Technology project under Grant Agreement No. 2023BAB052 by the Hubei Province 2023 Key R&D Program.

REFERENCES

[1] Lee JH, et al. Measurement and analysis on land-to-ship offshore wireless channel in 2.4 GHz. *IEEE Wireless Communications Letters*. 2017;6(2):222–225. DOI: 10.1109/lwc.2017.2662380.

[2] Wang W, Raulefs R, Jost T. Fading characteristics of ship-to-land propagation channel at 5.2 GHz. *OCEANS 2016 - Shanghai*. 2016; p. 1–7. DOI: 10.1109/OCEANSAP.2016.7485529.

[3] Zhang J, et al. Research on waterway wireless propagation characteristics based on channel measurement: Ship moving across vs. moving through. *Journal of Coastal Research*. 2020;99(sp1): 99. DOI: 10.2112/SI99-015.1.

[4] Bronk K, et al. Radio channel modelling for VHF system operating in the offshore wind farms propagation environment. *Sensors*. 2023;23(17):7593. DOI: 10.3390/s23177593.

[5] Balkees PAS, Sasidhar K, Rao S. A survey based analysis of propagation models over the sea. *2015 International Conference on Advances in Computing, Communications and Informatics (ICACCI)*. 2015; p. 69–75. DOI: 10.1109/ICACCI.2015.7275586.

[6] Gao Z, et al. Marine mobile wireless channel modeling based on improved spatial partitioning ray tracing. *China Communications*. 2020;17(3):1–11. DOI: 10.23919/JCC.2020.03.001.

[7] Yu J, et al. Measurement-based V2V radio channel analysis and modeling for bridge scenarios at 5.9 GHz. *IET Communications.* 2020;14(3):376-386. DOI: 10.1049/iet-com.2018.6274.

[8] Braga AD, et al. Radio propagation models based on machine learning using geometric parameters for a mixed city-river path. *IEEE Access*. 2020;8:146395-146407. DOI: 10.1109/ACCESS.2020.3012661.

[9] Eras LE, et al. A radio propagation model for mixed paths in Amazon environments for the UHF band. *Wireless Communications and Mobile Computing*. 2018. p. 1–15. DOI: 10.1155/2018/2850830.

[10] Ohta M, et al. Measurement experiments on 920 MHz band for spectrum sharing with LoRaWAN. *2018 IEEE 88th Vehicular Technology Conference (VTC-Fall)*. 2018. p. 1–5. DOI: 10.1109/VTCFall.2018.8690825.

[11] An F, Hu H, Xie C. Service network design in inland waterway liner transportation with empty container repositioning. *European Transport Research Review*. 2015;7(2). DOI: 10.1007/s12544-015-0157-5.

[12] Ai Q, et al. Joint optimization of USVS communication and computation resource in IRS-aided wireless inland ship MEC networks. *IEEE Transactions on Green Communications and Networking*. 2022;6(2):1023–1036. DOI: 10.1109/TGCN.2021.3135530.

[13] Li C, et al. Maritime broadband communication: Wireless channel measurement and characteristic analysis for offshore waters. *Journal of Marine Science and Engineering*. 2021;9(7):783. DOI: 10.3390/jmse9070783.

[14] Li F, et al. Ship-to-ship maritime wireless channel modeling under various sea state conditions based on REL model. *Frontiers in Marine Science*. 2023;10. DOI: 10.3389/fmars.2023.1134286.

[15] Yu J, et al. Path loss channel model for inland river radio propagation at 1.4 GHz. *International Journal of Antennas and Propagation*. 2017. DOI: 10.1155/2017/5853724.

[16] Yang K. Channel measurements and channel modeling for the open sea. *Norwegian University of Science and Technology*. 2015. http://hdl.handle.net/11250/2370724

[17] Molisch, AF. Wireless Communications. *John Wiley & Sons*; 2012.

[18] Beecraft L, Watson SB, Smith RE. Multi-wavelength pulse amplitude modulated fluorometry (Phyto-pam) reveals differential effects of ultraviolet radiation on the photosynthetic physiology of phytoplankton pigment groups. *Freshwater Biology*. 2016;62(1):72–86. DOI: 10.1111/fwb.12850.

[19] Deygout J. Correction factor for multiple knife-edge diffraction. *IEEE Transactions on Antennas and Propagation*. 1991;39(8):1256-1258. DOI: 10.1109/8.97368.

张祎，胡文飞，张俊武，张晶（通讯作者）

内河桥梁场景无线信道传播模型

摘要：
智能航运是交通运输系统的重要组成部分，而内河智能航运则是智能交通的重要保障。与陆地环境下的移动衰落信道研究相比，目前针对内河桥梁环境的信道测量和建模研究较少。本文提出了一种针对内河公铁两用桥的分段式无线电信道模型。船舶在桥下的路径被分为三个阶段，每个阶段的信号强度衰减分别建模。因此，它显示了不同区域的船对船无线信道以及内河航道桥梁上的路径损耗。相比于基本的路径损耗模型，分段模型可以准确预测路径损耗，为桥梁场景下的船对船无线信道传输提供了实用方法。因此，典型内河航道的信道测量和建模对建立可靠的内河航运无线电通信系统具有重要意义。

关键词：
船–船通信，无线通信，内河航道，无线信道特性，无线信道建模。